Available online at www.eccomasproceedia.org
Eccomas Proceedia SMART (2023) 169-180

ECCOMAS
Proceedia

X ECCOMAS Thematic Conference on Smart Structures and Materials
SMART 2023
D.A. Saravanos, A. Benjeddou, N. Chrysochoidis and T. Theodosiou (Eds)

VIBRATION SUPPRESSION OF LARGE FLEXIBLE STRUCTURES SUBJECTED TO TONAL EXCITATIONS VIA A SEMI-ACTIVE SHUNTED PIEZOELECTRIC TUNED MASS DAMPER

GRIGORIOS M. CHATZIATHANASIOU[1*], NIKOLAOS A. CHRYSOCHOIDIS[1] AND DIMITRIS A. SARAVANOS[1]

[1] Department of Mechanical Engineering & Aeronautics, University of Patras, Patras University Campus, 26500, Greece
[*] e-mail: chatziathanasiou.g@upnet.gr

Abstract. Multiple and altering tonal vibrations are common problem in flexible structures, such as lightweight means of transportation, induced by engine speed/rotor rotations, and their harmonics. A Semi-Active piezoelectric Tuned Mass Damper (SATMD) is developed for the suppression of these excitations, which consists of a resonant mass and a combined spring-piezoelectric device connected to an external resistive-inductive electric circuit. The proposed anti-vibration device introduces two anti-resonances to the host structure, which can be manipulated through changes in the shunt impedance, to highly suppress two dominating excitation frequencies or adjust the device to potential frequency fluctuations and maintain its performance. The vibration suppression capabilities of the SATMD are numerically and experimentally demonstrated on a down-scaled simplified airframe model. The anti-vibration device is experimentally proven to effectively adjust its performance to tonal frequency alterations, or to suppress two tonal excitations in distant frequency ranges, even in lower frequency vicinity than the initially tuned auxiliary mass. Finally, one tonal frequency and its 1st high amplitude harmonic are experimentally shown to be highly suppressed, using a SATMD which adds negligible mass to the structure.

Key words: Multiple tonal excitations, retuning, tuned mass damper, anti-resonance, piezoelectric, shunt circuit

1 INTRODUCTION

Forced tonal vibrations are a common problem in flexible structures such as lightweight means of transportation, where engines and rotors function under stationary or altering harmonic excitations. Some undesirable effects of tonal excitations are human discomfort and material wear due to fatigue. A great deal of research has been dedicated to address the reduction of tonal vibrations, including solutions such as structural redesign, passive, and active vibration control devices. More recently, semi-active adaptive vibration control devices have been vigorously studied, since they are able to perform under variable tonal excitations, without the need for excessive power supply. Shunt circuit piezoelectric patches have been studied for

Peer-review under responsibility of the organizing committee of SMART 2023.
doi: 10.7712/150123.9775.451064

their adaptive vibration control perfromance [1]-[2], since shunt impedance alterations can easily adjust the device tuning to the required bandwidth, without applying changes to its mechanical componenents.

A typical passive vibration control device comprises an auxiliary mass and a spring-damper element, and its structural parameters are tuned, such that a significant part of the host structure vibrations are mitigated to the auxiliary mass. When functioning under tonal vibrations, such devices are frequently names as tuned vibration absorbers (TVAs), whereas when functioning under broadband excitations, they are known as tuned mass dampers (TMDs). In this study, the term TMD will be used for all types of dynamic excitations. Since the pioneering work of Frahm [3], these devices have been widely investigated for their optimal characteristics [4], and applied in numerous civil engineering applications [5]-[6].

TMDs have also been studied for their adaptive control capabilities, since by altering their stiffness, e.g. changing the length of a pendulum TMD (PTMD) [7], they can cope with potential frequency fluctuations. TMDs comprising smart materials, such as shape memory alloys (SMAs) [8], and magnetorheological dampers [9], are also known for their capability to alter the TMD stiffness, therefore adjusting their vibration control efficiency to the required frequencies. Regarding the piezoelectric TMDs, several valuable research attempts have revealed their great potential for adaptive control [10]-[11], however most of the reported works do not demonstrate experimental results or validated models on flexible structures, and various voids and challenges remain open. Lately, a Semi-Active shunted piezoelectric TMD (SATMD), comprising a specialty piezoelectric device for suppressing low-frequency vibrations with negligible auxiliary mass, has been widely studied for multi-modal vibration control under broadband frequency excitation [12]-[13].

In this paper, the SATMD device is investigated for suppressing tonal frequency excitations on a lab-scale airframe model, and adapting its parameters to potentially large frequency alterations. This device introduces two highly tuneable anti-resonances to the host structure, which can be easily manipulated by the shunt circuit inductance. The main scientific contribution of the current study is the experimental demonstration of I) the adaptive suppression/ retuning capabilities of the proposed anti-vibration device, retaining its high vibration reduction performance, II) the high efficiency of the vibration control of two distant tonal excitations simultaneously, and III) the high perfromance of this damper in low frequency vicinities (lower than 160Hz), using an auxiliary mass less than 0.5% of the host structure mass, proving its application potential to real large and flexible structures. The rest of the paper is organized as follows: sections 2 and 3 describe the theoretical background and the experimental setup, respectively. The computational and experimental results are discussed in section 4, whereas some concluding remarks are summarized in section 5.

2 THEORETICAL BACKGROUND

Large flexible structures are typically modelled as equivalent discretized linear structure systems involving large numbers of degrees of freedom (DOFs) and complex system matrices. In the present work, the finite element method is used to synthesize the standard dynamic system of equations in the time domain,

$$M_{kl}\ddot{u}_l + C_{kl}\dot{u}_l + K_{kl}u_l = F_k \tag{1}$$

where: u is the vector of the N structural displacements, $\boldsymbol{M,K}$ represent the structural mass and stiffness matrices, respectively, $\boldsymbol{F}$ represents the applied external loads, and $k,l = 1,...,N$ is the respective DOF. The structural damping matrix $\boldsymbol{C}$ is either directly calculated from material damping coefficients, or from measured modal damping values, as explained below.

In order to focus on the vibration analysis of a small subset of X modes excited by aerodynamic loads within a low frequency range, and at the same time reduce the large size of the structural system, transformation to the modal space is a commonly followed strategy. Integrating the SATMD to the host structure and assuming that its auxiliary mass, damping, and stiffness are too small to alter the mode shapes of the host structure, the integrated system equations are formulated as:

$$\begin{bmatrix} \bar{\boldsymbol{M}} & \boldsymbol{0} & \boldsymbol{0} \\ \boldsymbol{0} & m_d & 0 \\ \boldsymbol{0} & 0 & L \end{bmatrix} \begin{Bmatrix} \ddot{\boldsymbol{Q}} \\ \ddot{u}_d \\ \ddot{q}_2 \end{Bmatrix} + \begin{bmatrix} \bar{\boldsymbol{C}} + c_d \boldsymbol{\Phi_n}^T \boldsymbol{\Phi_n} & -c_d \boldsymbol{\Phi_n}^T & \boldsymbol{0} \\ -c_d \boldsymbol{\Phi_n} & c_d & 0 \\ \boldsymbol{0} & 0 & R \end{bmatrix} \begin{Bmatrix} \dot{\boldsymbol{Q}} \\ \dot{u}_d \\ \dot{q}_2 \end{Bmatrix} + \begin{bmatrix} \bar{\boldsymbol{K}} + k_p \boldsymbol{\Phi_n}^T \boldsymbol{\Phi_n} & -k_p \boldsymbol{\Phi_n}^T & \frac{\bar{e}}{C_p} \boldsymbol{\Phi_n}^T \\ -k_p \boldsymbol{\Phi_n} & k_p & -\frac{\bar{e}}{C_p} \\ \frac{\bar{e}}{C_p} \boldsymbol{\Phi_n} & -\frac{\bar{e}}{C_p} & \frac{1}{C_p} \end{bmatrix} \begin{Bmatrix} \boldsymbol{Q} \\ u_d \\ q_2 \end{Bmatrix} = \begin{Bmatrix} \boldsymbol{P} \\ 0 \\ 0 \end{Bmatrix} \quad (2)$$

where: $\boldsymbol{Q}$ is the vector of the modal participation factors of the host structure, such that $\{u\}_{Nx1}=[\Phi]_{NxX}\{Q\}_{Xx1}$, where Φ is the modal matrix of the X undamped eigenvectors. $\bar{\boldsymbol{M}},\bar{\boldsymbol{K}}$ are the modal mass and stiffness diagonal matrices respectively, $\boldsymbol{P}$ is the modal force, $\bar{\boldsymbol{C}}$ is the modal damping matrix (assumed to be diagonal and synthesized from measured modal damping values of the baseline structure). m_d is the auxiliary mass of the damper, u_d is its displacement, c_d is the lumped damping and k_p the equivalent piezoelectric stiffness of the piezoelectric device, where $k_p = k_d + \frac{\bar{e}^2}{C_p}$. q_2 is the shunt circuit charge, $\bar{e}$ and C_p the equivalent piezoelectric coefficient and capacitance of the piezoelectric transducer, and R, L the shunt resistance and inductance, respectively. Finally, n is the structural DOF of the structure, where the SATMD is attached, so Φ_n is a line-vector, where each element is the amplitude of the respective mode shape of the n DOF. The derivation of Eq. (2) and the integration of the SATMD characteristics are thoroughly analysed in [13].

As seen in Eq. (2), the inductance adds a new complex conjugate pair of roots into the system, which corresponds to an additional dominant electrical mode. Depending on the strength of electromechanical coupling, the electrical mode is not purely electrical and may contain strong mechanical components from mechanical DOFs of the host structure and the auxiliary mass, and vice versa. As shown in [13], this electromechanical mode is evident on the host structure as a close pair of resonance and anti-resonance, whose frequency vicinity is highly dependent on the variable inductance. Furthermore, the inductance highly affects the auxiliary mass anti-resonance, altering its effective mass, and shifting it to lower frequency ranges. The manipulation of these two anti-resonances, via simple shunt circuit alterations (adding or removing a coil for inductance variation), yields the capability of the proposed anti-vibration device to retune its performance according to the system frequency fluctuations, or simultaneously tune its anti-resonances and suppress two tonal excitations.

3 EXPERIMENTAL SETUP

The experimental setup consists of a down-scaled airframe prototype and the proposed anti-vibration device for tonal excitations (SATMD). The SATMD comprises an auxiliary mass and a specialty piezoelectric device, which provides the stiffness for the auxiliary mass and introduces high electromechanical coupling, connected to an external resistive-inductive (RL) shunt circuit.

3.1 Lab-Scale Airframe Structure

A simplified structural dynamics model of a small regional aircraft (Fig. 1a) was scaled down to accommodate lab-dimensions, while maintaining similarity in dynamic characteristics. The protype was fabricated having a total mass of approximately 112kg and consists of the following components: (i) a 3m steel tubular beam representing the aircraft fuselage; (ii) two aluminum plate-strips for the wings and the horizontal tail stabilizer, respectively; and (iii) three plastic connectors for the mounting of the wings, the horizontal tail, and the proposed damper, respectively. The dimensions, materials, properties, and boundary conditions can be found in [13].

The simplified aircraft prototype was excited via an LDS electromechanical shaker, with up to 200N loading capacity, mounted at the middle of the horizontal tail. A load cell was intervened between the shaker stinger and the tested structure. Accelerations normal to the plane of the tested structure were measured at the fuselage tip and center. A high speed DAQ board was used to perform the testing campaign operating on NI LabVIEW platform. To obtain the frequency response of the structure, The actuation signal was a white noise signal with frequency bandwidth up to 2048Hz, generated on LabVIEW, converted to analog, amplified, and finally driven to the shaker to continuously excite the structure. The time signals of the applied force from the actuator as well as the accelerations were simultaneously acquired via the DAQ board.

a.  b. 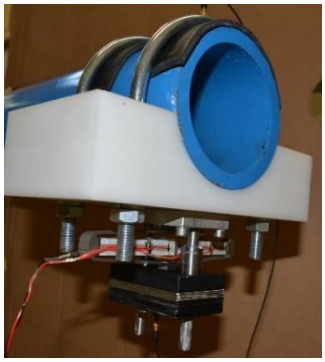

Figure 1. Experimental Setup: (a) Down-scaled airframe model; (b) Piezoelectric device attached under fuselage tip in vertical direction.

For the simulation, a detailed finite element model was developed in Abaqus software using 4-node reduced integration shell elements for both the tubular steel beam and the aluminum wings and tail (1406 nodes in total). The undamped eigenvectors of the host structure, the modal masses and modal stiffnesses, were extracted from the modal analysis executed in Abaqus. All structural modes from 30Hz to 180Hz are used in the mode superposition model of Eq. 2. The

measured modal damping values of the baseline structure were included in the modal damping matrix of the reduced system Eq. 2. The modal characteristics of the structure are shown in Table 1. Results of the mode superposition analysis are compared to experimental measurements for the fuselage tip Baseline (no SATMD attached) in Fig. 2a. The studied host structure exhibits four strong eigenfrequencies at 36Hz, 47Hz, 64Hz and 158Hz, as observed in Fig. 2a. Great agreement is achieved between the experiment and simulation results, validating the developed model.

Table 1. Modal Characteristics of the studied modal frequencies

	Frequency [Hz]	**Mass[kg]**	**Damping [Ns/m]**	**Stiffness [kN/m]**
1	35.9	3.1	3.7	156.9
2	47.0	12.4	18.0	1076.0
3	64.4	0.6	1.9	100.5
4	78.9	4.0	2.0	976.5
5	103.2	2.4	3.0	1010.4
6	158.8	17.1	45.0	17019.2

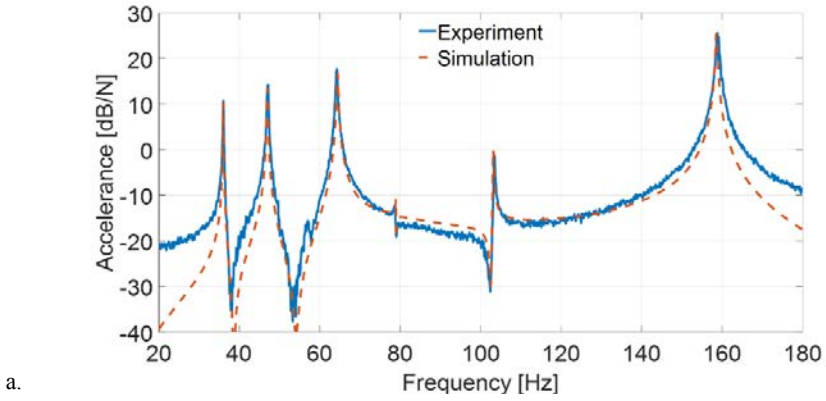

a.

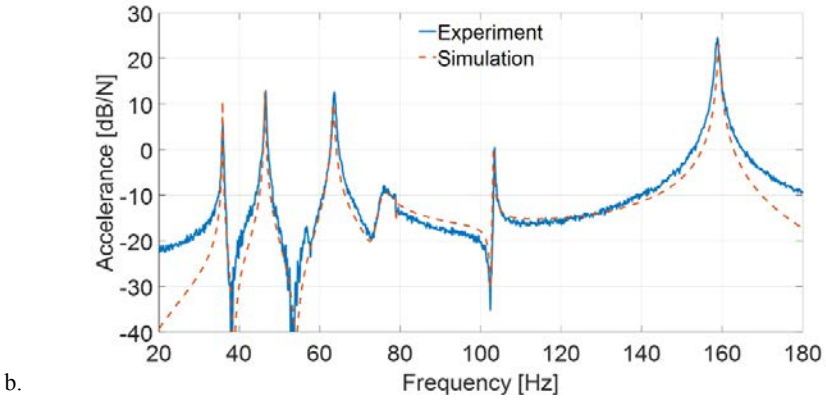

b.

Figure 2. Experiment – Model frequency response of the airframe tip: (a) Without the SATMD; (b) With the SATMD.

3.2 Piezoelectric device, shunt circuit, and auxiliary mass

The piezoelectric device for the electromechanical SATMD is a specialty diamond-shaped piezoelectric transducer, whose terminals are shunted to a circuit with electrical impedance.

The transducer consists of two big piezoelectric stacks and a stroke amplifying frame, which also provides the equivalent mechanical stiffness. The piezoelectric device can convert significant part of the kinetic energy into electrical energy and consequently direct it in the shunting circuit. At the same time the selected piezoelectric transducer requires a relatively small auxiliary mass, to mechanically tune the damper to relatively low frequencies. The concerns of brittleness and failure are addressed with the adopted actuator mechanism, which encapsulates the piezoelectric stack in the frame under pre-compression. The static loading of the actuator by the auxiliary mass further enhances the compression of the piezoelectric stack. Moreover, to restrict the auxiliary mass to axial movement, a combination of vertical guides and linear bearings was designed and applied.

For the piezoelectric device model, an equivalent lumped parameter spring-piezoelectric device model is assumed, whose equivalent characteristics are calibrated as shown in [13], and presented in Table 2. The SATMD was decided to be attached under the tubular beam tip (Fig. 1b).

Table 2. Piezoelectric device characteristics.

Auxiliary mass m_d [kg]	0.46
Equivalent total Damping c_d [Ns/m]	7
Equivalent mechanical Stiffness k_d [kN/m]	100
Equivalent piezoelectric coefficient $\bar{e}$ [N/V]	0.65
Capacitance C_p [μF]	27

Considering the external circuit impedance, the resistance is controlled by an easily tunable potentiometer, whereas variable inductive loads are introduced by connecting in-series low cost, low-weight, commercially available coils, making them efficient and suitable for a real application. To ensure that the shunt impedance is correctly applied in the analytical model, the resistance of each coil combination was measured using a RLC meter.

Tonal frequencies are generally applied away from the high amplitude structural modes, however potential frequency fluctuations may excite these modes as well. For this reason, in this experimental campaign, the auxiliary mass was selected at 460g, to tune the short circuit device (Passive TMD behavior) away from the host structure eigenfrequencies (anti-resonance at 73Hz). The impedance of the SATMD shunt circuit will improve the performance of the anti-vibration device to tonal excitations via two mechanisms: A) it will adjust the tuning of the device to the host structure eigenfrequencies, by altering the effective auxiliary mass, and B) it will introduce a second electromechanical resonator, to simultaneously suppress another tonal excitation.

To validate the developed model, the experimental measurements of the studied Passive TMD are compared to the respective results of the mode superposition analysis in Fig. 2b, demonstrating great agreement. The addition of the Passive TMD to the structure affects only a narrow bandwidth around the targeted frequency (73Hz), while the rest of the frequency response exhibits similar behavior to the Baseline.

4 RESULTS AND DISCUSSION

4.1 Explicit Inductance Effect

The scope of this section is to thoroughly study the effect of the undamped electromechanical pole (R=0) introduced by pure inductance. Added resistance would dissipate the energy and introduce damping to the results, potentially diminishing the anti-resonances. This investigation contributes to the complete understanding of the enhancement of electromechanical coupling and the exploitation of the anti-resonance introduced by the electrical resonator. However, it is impossible to find ideal coils with zero resistance, thus the experimental study with similar inductance values, and resistance, is presented in the next sections.

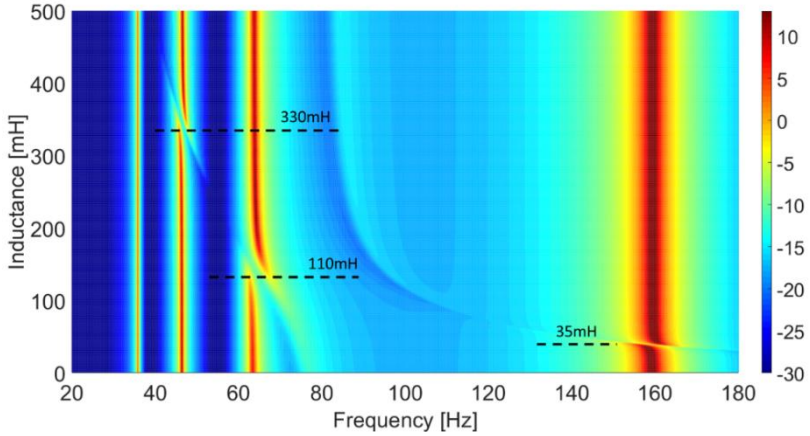

Figure 3. Inductance effect on the frequency response functions of the fuselage tip acceleration

The effect of inductive impedance on the FRF of the airframe tip acceleration is illustrated in Fig. 3. This surface plot can be intuitively understood as the frequency response of the airframe tip that corresponds to various inductance values. The frequency peaks are indicated by the red and yellow colors, whereas the blue areas imply lower amplitude of vibrations.

For zero and very small inductance in Fig. 3, the auxiliary mass anti-resonance is evident from the blue color area at 73Hz, and the frequency response of the structure is as described in Fig 2b. The electromechanical mode and respective anti-resonance exhibit larger frequency values than the plot frequency bandwidth and is therefore not evident. As the inductance increases, the electromechanical mode and respective anti-resonance approaches lower band vicinities, appearing near 180Hz, and crossing the 158Hz structural mode at 35mH, highly reducing its amplitude. At the same time, the auxiliary mass anti-resonance is shifted to lower frequency vicinities, progressively approaching the 64Hz structural mode, until crossing it, and as a result, highly suppressing it, at approximately 110mH. For higher inductance values, the two anti-resonances remain distinct in frequency, as depicted in Fig. 3, however the electrical pole continues in lower frequency bandwidth. As a result, the lower frequency anti-resonance is now attributed to the electrical mode, whereas the higher to the auxiliary mass. For inductance higher than 110mH, the electromechanical anti-resonance approaches the area of 80Hz, depicted by the light blue curve, while the auxiliary mass anti-resonance approaches and finally crosses the 47Hz structural mode at approximately 330mH.

These computational results paved the way for experimental campaign, where the inductance of the available coils is employed, along with their intrinsic resistance, and the experimental measurements are demonstrated in the following sections.

4.2 Experimental Inductance-Resistance Effect

The experimental results of the frequency response of the airframe tip with the SATMD, passively tuned to 73Hz, and a shunt circuit comprised of various coil combinations, along with their intrinsic resistance, are illustrated in Figs 4. The studied impedance values on each figure are selected for better visualization purposes, such that the respective curves are distinct in the desired frequency ranges.

For 30mH (green curve in Fig. 4a), the mechanical anti-resonance is shifted to slightly lower frequency bandwidth, whereas the electromechanical mode and respective anti-resonance is close to the 158Hz structural mode, lowering its amplitude. The resistance of the coil, along with the extremely sensitive electromechanical resonance (small inductance changes lead to big frequency fluctuations of the electromechanical mode), and the fact that the available coils exhibit minimum inductance of 10mH, making the exact tuning to 35mH impossible, lead to the invisibility of the electromechanical anti-resonance.

For 50mH (orange curve in Fig. 4b), the mechanical anti-resonance is shifted to 70Hz, whereas the electromechanical anti-resonance is shifted to lower frequency than the 158Hz, where no structural mode exists and therefore is not visible.

For 110mH (yellow curve in Fig. 4b), the mechanical anti-resonance is shifted close to the 64Hz structural mode, highly reducing its amplitude. The higher values of resistance add damping to the results and diminishing the anti-resonance effect. The electromechanical mode and respective anti-resonance are not visible for the same reason as before.

For 330mH (dashed red curve in Fig. 4a), the lower anti-resonance is shifted close to the 47Hz structural mode, highly reducing its amplitude. The higher anti-resonance has approached the short circuit anti-resonance and is evident close to 80Hz.

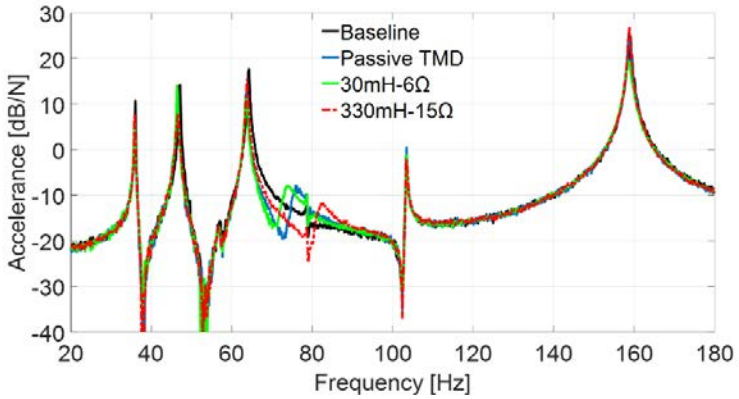

a.

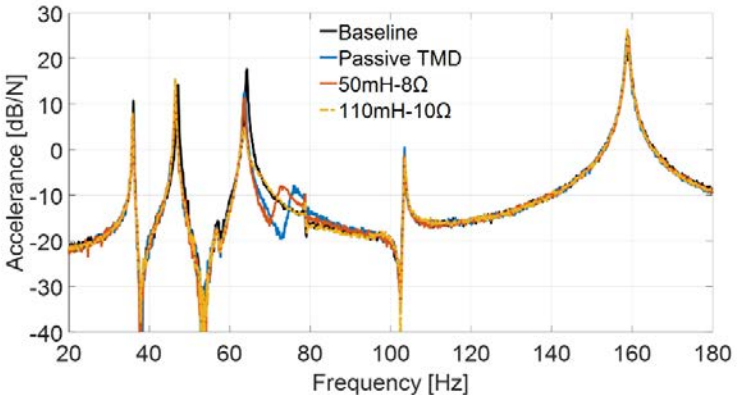

b.

Figure 4. Experimental frequency response of the airframe tip under various SATMD impedance values.

4.3 Case Studies

4.3.1 SATMD Retuning

To exploit the retuning capabilities of the studied SATMD device, a tonal excitation is supposed to exhibit a fluctuation from 73Hz to 70Hz, thus retuning is required for maintaining the highest possible vibration control. The results in the time domain illustrated in Fig. 5 for tonal excitation at 70Hz demonstrate that the passive TMD at 73Hz (blue curve) reduces the acceleration amplitude; however better performance is achieved with the selected SATMD (orange curve).

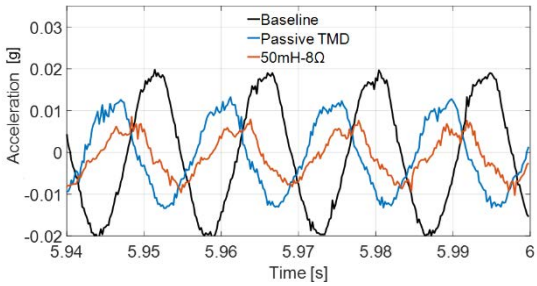

Figure 5. Tip acceleration in time domain under tonal excitation at 70Hz.

4.3.2 SATMD Suppressing two tonal frequencies

The simultaneous reduction of vibration in two tonal frequencies is studied for two different cases. Each case focuses to one structural mode, since these frequencies are expected to exhibit high amplitude vibrations, and measures against such occasions should be taken.

I) 70Hz and 158Hz

Two tonal excitations are induced to the lab-scale airframe at 70Hz and 158Hz. Applying the SATMD with the studied auxiliary mass and shunt circuit of 30mH and 6Ω (green curve in Fig. 4a), both tonal vibrations are reduced via the electromechanical and auxiliary mass antiresonances. Fig. 6a illustrates the time domain measurements without (black curve) and with the SATMD (green curve). To quantify the vibration reduction in each one of these two tonal frequencies, fast Fourier Transformation (FFT) is applied to the measured acceleration

signals, and the respective results are illustrated in Fig. 6b, showing great vibration reduction in each tonal frequency.

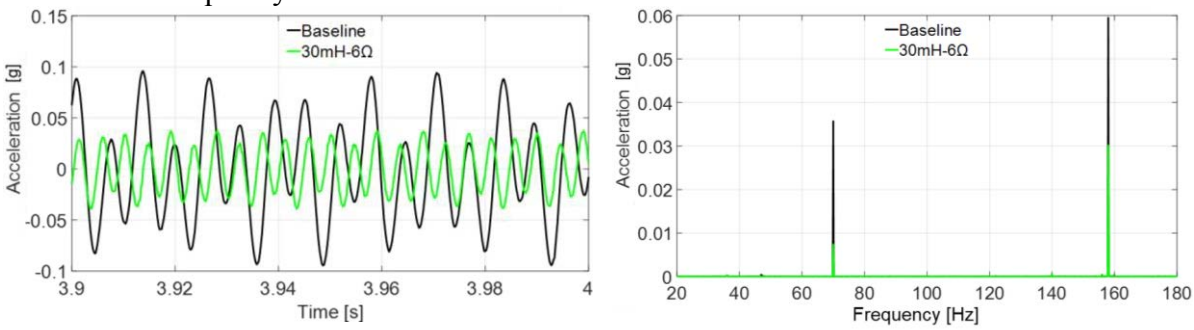

a. b.

Figure 6. Tip acceleration under tonal excitations at 70Hz and 158Hz in: (a) Time domain; (b) Frequency domain.

II) 47Hz and 80Hz

As a second case study in the vibration suppression of two simultaneous tonal vibrations, with one being in much lower frequency than the passive damper, two tonal excitations are induced at 47Hz and 80Hz. Applying the SATMD with the studied auxiliary mass and shunt circuit of 330mH and 15Ω (red curve in Fig. 4a), both tonal vibrations are reduced. Similar to the previous case, the experimental results are illustrated in the time and frequency domain in Figs. 7a, b, where the 47Hz excitation is highly attenuated (over 70%). A remarkable note regarding this case study is that, having a conventional TMD with the same stiffness as the studied piezoelectric device, the auxiliary mass needed to tune the TMD to 47Hz would be 1.14kg, that is almost 2.5 times the studied 460g auxiliary mass.

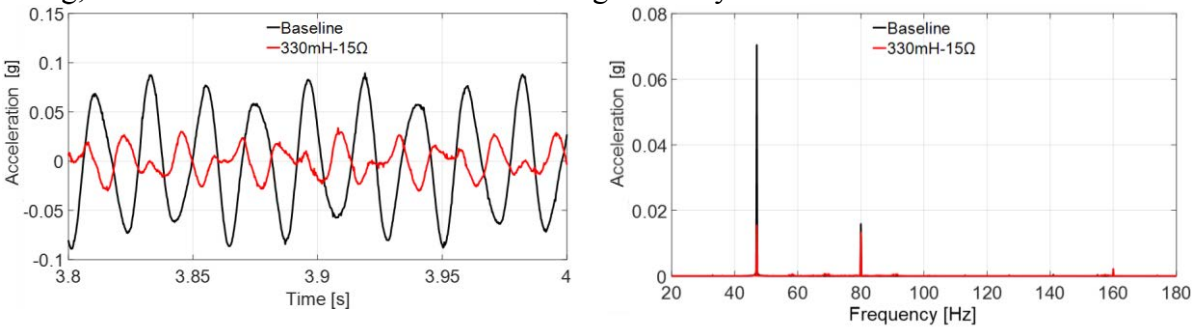

a. b.

Figure 7. Tip acceleration under tonal excitations at 47Hz and 80Hz in: (a) Time domain; (b) Frequency domain.

4.3.3 SATMD Suppressing one tonal and its high amplitude harmonic

To study the effects of the harmonics of one tonal excitation in the studied host structure, and the performance of the SATMD to both vibrations, the 158Hz structural mode is excited, as the 1st harmonic vibration of a tonal frequency at its half frequency, thus at 79Hz. To simultaneously achieve that both the device anti-resonances are tuned close to 79Hz and 158Hz, an auxiliary mass of 350g was chosen, to initially tune the passive damper to 84Hz (purple

curve in Fig. 8), and 30mH inductance is applied, along to its intrinsic resistance (light blue curve in Fig. 8).

Fig. 9a illustrate the time domain experimental measurements without (black curve) and with the SATMD (light blue curve), while Fig. 9b their FFT transformations to the frequency domain. As shown in both Figs. 9, both the tonal frequency and its 1st harmonic are satisfactorily reduced, demonstrating the SATMD capabilities.

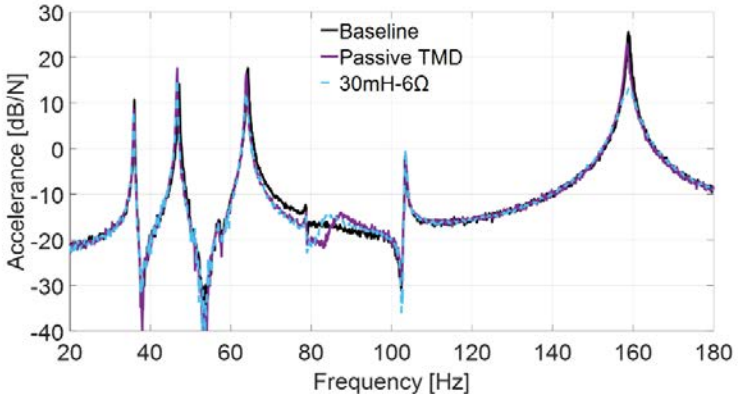

Figure 8. Experimental frequency response of the airframe tip under Passive TMD and SATMD.

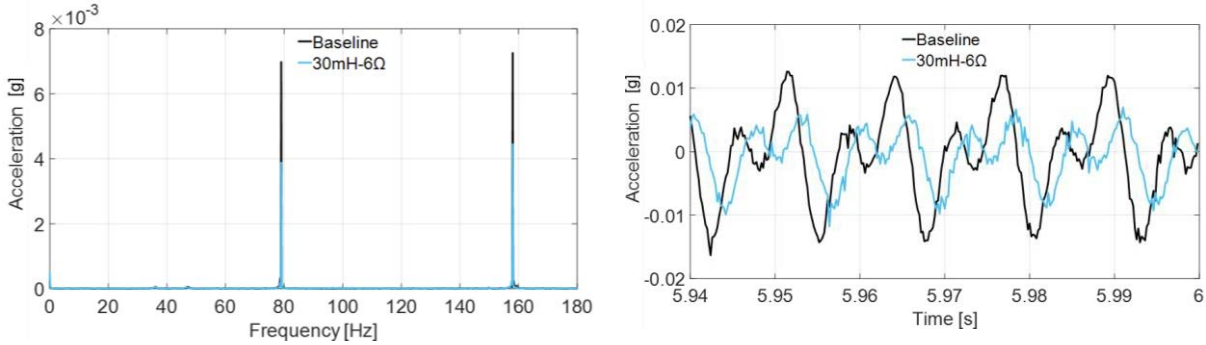

a. b.

Figure 9. Tip acceleration under tonal excitation at 79Hz, yield a high amplitude 1st harmonic vibration at 158Hz in: (a) Time domain; (b) Frequency domain.

5 CONCLUSIONS

The shunted piezoelectric SATMD presented in this work was investigated to suppress tonal vibrations in a large flexible structure, and to adapt to variable frequency fluctuations. The SATMD introduces two highly tunable anti-resonances, dictated by the shunt circuit inductance, and affecting the host structure in variable frequency spectrums. Having a validated truncated mode superposition model of the studied lab-scale airframe, a computational analysis suggested the appropriate inductance levels to tune the anti-vibration device to new frequencies. The experimental measurements showed that the SATMD can be retuned to cope with potential frequency fluctuations and suppress two distinct tonal excitations simultaneously. The specialty piezoelectric device allowed for a small auxiliary mass (smaller than 0.5% of the host structure total mass) to achieve satisfactory vibration reduction results to a frequency bandwidth up to

160Hz. Another remarkable outcome was the ability of the SATMD to tune its anti-resonance to a much lower structural mode, compared to the mechanically tuned damper, which would require 2.5 times the studied auxiliary mass. Finally, the results showed high sensitivity of performance to the auxiliary mass, inductance and damping introduced by resistance. As a result, parameter optimization along with higher quality experimental setup is expected to yield higher vibration attenuation performance.

REFERENCES

[1] N. W. Hagood and A. von Flotow, "Damping of structural vibrations with piezoelectric materials and passive electrical networks," *J. Sound Vib.*, vol. 146, no. 2, pp. 243–268, 1991, doi: https://doi.org/10.1016/0022-460X(91)90762-9.

[2] J. J. Hollkamp and T. F. Starchville, "A Self-Tuning Piezoelectric Vibration Absorber," *J. Intell. Mater. Syst. Struct.*, vol. 5, no. 4, pp. 559–566, 1994, doi: 10.1177/1045389X9400500412.

[3] F. H. (DE), "DEVICE FOR DAMPING VIBRATIONS OF BODIES.," no. 0989958. 1911, [Online]. Available: https://www.freepatentsonline.com/0989958.html.

[4] "Mechanical Vibrations. Fourth Edition. J. P. Den Hartog. McGraw-Hill, New York, 1956. 67s. 6d.," *J. R. Aeronaut. Soc.*, vol. 61, no. 554, pp. 139–139, Feb. 1957, doi: 10.1017/S0368393100131049.

[5] S. Elias and V. Matsagar, "Research developments in vibration control of structures using passive tuned mass dampers," *Annu. Rev. Control*, vol. 44, pp. 129–156, 2017, doi: 10.1016/j.arcontrol.2017.09.015.

[6] N. Debnath, S. K. Deb, and A. Dutta, "Multi-modal vibration control of truss bridges with tuned mass dampers under general loading," *J. Vib. Control*, vol. 22, no. 20, pp. 4121–4140, Feb. 2015, doi: 10.1177/1077546315571172.

[7] L. Wang, W. Shi, X. Li, Q. Zhang, and Y. Zhou, "An adaptive-passive retuning device for a pendulum tuned mass damper considering mass uncertainty and optimum frequency," *Struct. Control Heal. Monit.*, vol. 26, no. 7, pp. 1–21, 2019, doi: 10.1002/stc.2377.

[8] K. A. Williams, G. T. Chiu, and R. J. Bernhard, "ARTICLE IN PRESS Dynamic modelling of a shape memory alloy adaptive tuned vibration absorber," vol. 280, pp. 211–234, 2005, doi: 10.1016/j.jsv.2003.12.040.

[9] F. Weber, "Semi-active vibration absorber based on real-time controlled MR damper," *Mech. Syst. Signal Process.*, vol. 46, no. 2, pp. 272–288, 2014, doi: 10.1016/j.ymssp.2014.01.017.

[10] C. L. Davis and G. A. Lesieutre, "Actively tuned solid-state vibration absorber using capacitive shunting of piezoelectric stiffness," *J. Sound Vib.*, vol. 232, no. 3, pp. 601–617, 2000, doi: 10.1006/jsvi.1999.2755.

[11] M. Lallart, L. Yan, Y. C. Wu, and D. Guyomar, "Electromechanical semi-passive nonlinear tuned mass damper for efficient vibration damping," *J. Sound Vib.*, vol. 332, no. 22, pp. 5696–5709, 2013, doi: 10.1016/j.jsv.2013.06.006.

[12] G. M. Chatziathanasiou, N. A. Chrysochoidis, and D. A. Saravanos, "A semi-active shunted piezoelectric tuned mass damper for robust vibration control," *J. Vib. Control*, no. May, p. 107754632110264, 2021, doi: 10.1177/10775463211026487.

[13] G. M. Chatziathanasiou, N. A. Chrysochoidis, C. S. Rekatsinas, and D. A. Saravanos, "A semi-active shunted piezoelectric tuned-mass-damper for multi-modal vibration control of large flexible structures," *J. Sound Vib.*, vol. 537, no. June, p. 117222, 2022, doi: 10.1016/j.jsv.2022.117222.